Development and characterization of fish myofibrillar protein/chitosan/rosemary extract composite edible films and the improvement of lipid oxidation stability during the grass carp fillets storage

Development and characterization of fish myofibrillar protein/chitosan/rosemary extract composite edible films and the improvement of lipid oxidation stability during the grass carp fillets storage

Hongying Du[a, b,*]; Chen Liu[a]; Ozan Unsalan[c]; Çisem Altunayar Unsalan[d]; Shanbai Xiong[a, b]; Anne Manyande [e]; Hongli Chen[f,*]

[a] Key Laboratory of Environment Correlative Dietology, Ministry of Education, College of Food Science and Technology, Huazhong Agricultural University, Wuhan, Hubei, P.R. China

[b] National R & D Branch Center for Conventional Freshwater Fish Processing, Wuhan, Hubei 430070, P.R. China

[c] Ege University, Faculty of Science, Department of Physics, 35100, Bornova, Izmir, Turkey

[d] Ege University Central Research Testing and Analysis Laboratory Research and Application Center, 35100, Bornova, Izmir, Turkey

[e] School of Human and Social Sciences, University of West London, Middlesex TW8 9GA, UK

[f] State Key Laboratory of Applied Organic Chemistry, College of Chemistry and Chemical Engineering, Key Laboratory of Nonferrous Metal Chemistry and Resources Utilization of Gansu Province, Lanzhou University, Lanzhou, 730000, China

* Corresponding author

Hongying Du: Email: hydu@mail.hzau.edu.cn;

Hongli Chen: Email: hlchen@lzu.edu.cn

Abstract: Biofilm composition from fish myofibrillar protein (FMP) and chitosan solution (CS) incorporated with rosemary extract (RE) was developed and applied to monitor the freshness of fish fillets. The effects of different concentrations of RE (0.05%，0.1%，0.15%，0.2%, *v*/*v*) as well as physical, mechanical, structural and functional properties of FMP/CS films were investigated. Films containing RE showed reduced water solubility and water vapor permeability (WVP) and enhanced tensile strength and elongation at break. Results of X-ray diffraction (XRD), scanning electron microscopy (SEM) and atomic force microscopy (AFM) suggest that there was good compatibility of the components and good dispersion of RE in the matrix. However, the content of RE (0.2%, *v*/*v*) added in the composite films produced aggregations and had negative effects on their film-forming properties. The antioxidant capacity of composite films was related to the level of RE and demonstrated by the DPPH (2,2-diphenyl-1-picrylhydrazyl) free radical scavenging assay. Chilled grass carp fillets wrapped with different films to evaluate the preservative effect were stored at 4 °C. Results of thiobarbituric acid reactive substances (TBARS), pH value, Free amino acid (FAA) and total volatile basic nitrogen (TVB-N) indicated that FMP/CS/RE composite film could protect the fish fillet well and inhibit the lipid oxidation. In summary, the developed FMP/CS/RE composite films possess the potential to be applied as edible films in the food packaging industry and food cold chain transportation.

Keywords: Fish myofibrillar protein; Rosemary extract; Composite edible films; Biofilm composition;

1. Introduction

During the past decade, composite edible films and packaging have drawn more attention due to their excellent barrier, edibility, renewable and biodegradable properties compared with their synthetic counterparts [1]. Various natural resources such as polysaccharides, proteins, lipids and carbohydrates are often used to develop environmentally friendly biopolymer films [2]. Proteins are one of the biopolymer materials empirically used as edible food packaging materials on account of their good film-forming ability [3]. To enhance the mechanical and physicochemical properties of edible films, proteins are usually mixed with polysaccharides, carbohydrates, polyphenols *etc*. [4-6].

Myofibrillar protein (MP) is a popular protein-based hydrophilic polymer extract from aquatic products. Fish myofibrillar protein (FMP) can form a continuous matrix during the drying process, which can be used to prepare transparent films with certain mechanical properties. However, due to the existence of disulfide bonds, hydrogen bonds, electrostatic forces and hydrophobic interactions in intermolecular MP, the individual MP-based biofilm is more fragile. Therefore, some researchers have focused on the modification of FMP-based edible films by adding different kinds of additives. FMP-based films incorporated with procyanidins and tea polyphenol could improve the thermal stability and rigidity of films [7]. FMP based film modified with phenolic compounds suggest stronger and stiffer film structure by allowing crosslinking of MP and polyphenols [8]. Bacterial cellulose nanofibers were employed in order to reinforce the various properties of edible FMP nanocomposite films [9]. Furthermore, technological properties were improved by adding chitosan solution (CS) to MP based films [10].

Presently, rosemary extract (RE) is widely used in the inhibition of lipid oxidation, meat and

aquatic products preservation. For example, the application of RE in glazing treatment on preservation of mud shrimp significantly reduced loss of quality protein and lipid changes [11]. RE is also useful in decreasing quality loss and inhibiting lipid oxidation of minced sea salmon muscles during frozen storage [12], inhibiting lipid oxidation and maintaining color stability during storage of beef burgers [13]. Furthermore, there are many more papers in which RE was added to the edible film. For example, when RE was added to the cellulose/gelatin hydrolysate composite film it improved the mechanical and ultraviolet light barrier properties of the film [14]. The oxidative and microbial stability of smoked eel fillets were also enhanced by the edible coating enriched with RE [15].

However, there is few reports with regards to the application of RE to FMP/CS composite film. In this study, the modification of RE to FMP/CS composite film and the corresponding properties including mechanical properties, water solubility, light transmittance, water vapor transmission rate and morphology features were measured. Meanwhile, the effects of RE on the microstructure of FMP/CS composite film were further explored using X-ray diffraction (XRD), scanning electron microscopy (SEM) and atomic force microscopy (AFM). Moreover, the quality changes and lipid oxidation during inhibition of fresh fish fillets wrapped with FMP/CS/RE composite film, polyvinyl chloride (PVC) film and the untreated group were investigated and compared. The developed composite films possess the potential to be applied as edible films in the food packaging industry and food cold chain transportation.

2. Materials and methods

2.1 Materials

The fresh grass carp (~ 2.5 kg) was purchased from the local market in Huazhong Agricultural

University (Hubei, China). The fish were gutted, cleaned, filleted and mechanically deboned. The dorsal white muscle samples were frozen in liquid nitrogen and kept at −80 °C until used for MP extraction. Chitosan with 90% degree of deacetylation was purchased from Sinopharm Chemical Reagent Co., Ltd. (Shanghai, China). RE was obtained from Hangzhou Linran Biotechnology Co., Ltd. (Purity 80%, Hangzhou, China). All other reagents used in the present study were of analytical grade and acquired from Sinopharm Chemical Reagent Co., Ltd. (Shanghai, China).

2.2 Myofibrillar Protein extraction

MP was extracted from grass carp as described in our previous work [16]. Briefly, dorsal white fish muscle was minced and rinsed in a low-salt phosphate buffer (0.05 mmol/L NaCl, 3.38 mmol/L NaH_2PO_4, 15.5 mmol/L Na_2HPO_4, pH 7.5) in order to remove the water-soluble protein and other substances using a homogenizer (T18 digital ULTRA TURRAX, IKA, Germany) at a speed setting of 9000 *g* for 1 min. The homogeneous liquid was further centrifuged at 8000 *g* for 5 min by a refrigerated centrifuge (4 °C, Avanti J-26 XP, Beckman Coulter, CA, USA). Then the obtained pellets were extracted at 4 °C in a high salt phosphate buffer (0.45 mmol/L, pH 7.5). After centrifugation, the supernatant was poured into deionized water at 4 °C to precipitate MP. Finally, the precipitate (MP) was collected by centrifugation, then diluted with 0.6 M NaCl Tris–HCl (pH 7.5) buffer and kept in a fridge at 4 °C for further analysis. The MP concentration was determined by the Lowry method [17], with serum albumin used as the standard. The purity of MP was about 8% (*w*/*v*).

2.3 Edible film preparation

The edible film-forming solution was prepared according to a previous method [18] with little modification. Distilled water was added to MP to obtain the protein concentration at 2% (*w*/*v*), then

110 homogenized at 9000 *g* for 1 min and the pH was adjusted to 3.0 with 1 M HCl. It was centrifuged
111 at room temperature with a centrifugal force of 3000 *g* for 10 min and then the supernatant was
112 collected. Glycerol was added as a plasticizer to the solutions at a concentration of 1.63% (*w*/*v*) and
113 stirred at room temperature for 30 min. Chitosan was dissolved in 1% acetic acid to get the chitosan
114 fully dissolved, and stirred overnight to make the final 2% CS. Finally, the solution was mixed with
115 CS using a homogenizer to obtain the MP/CS (4.33:3.67) composite film forming solution,
116 according to previous results of response surface optimization (data not shown).

117 To ensure full hydration of the biopolymer dispersions (MP, CS, and MP/CS), the dispersions
118 were mixed together and homogenized for 30s [18] Then, different amounts of RE were added to
119 achieve the final volume ratios of 0.05%，0.1%，0.15%，0.2% similar to the former mixture of
120 composite film (MP/CS). After mixing evenly, a volume of 40 mL of each film-forming solution
121 was cast in polystyrene petri dishes (13 cm diameter), dried at 50 °C for 16 h. The edible composite
122 films were stored in a desiccator at 25 °C and 50% relative humidity (RH) for 24 h. Dried films
123 were manually peeled off from the surface for further analysis.

124 **2.4 Film thickness and mechanical properties**

125 Film thickness was determined using digital micrometer (PosiTector 6000, DeFelsko
126 Corporation, USA) with a precision of 0.001 mm. Five measurements at different positions were
127 taken from each film sample to obtained the mean film thickness[19]. These measurements were
128 obtained after a conditioning period at 25 °C with a relative humidity of 50%. Tensile strength (TS,
129 MPa) and elongation at break (EB, %) of film samples were determined as formerly described [7],
130 using a Texture Analyzer (TA.XT.plus, Stable Micro Systems, UK). The films were cut into 50
131 mm×20 mm strips, then the initial grip separation and cross-head speed were set at 30 mm and 2

mm/s, respectively. TS was calculated by dividing the maximum force with the initial cross-sectional area of the film; EB (%) was calculated by dividing the film elongation at break with the initial gauge length of the specimen.

2.5 Determination of moisture content and water solubility

Film samples (4×4 cm^2) were prepared and weighed (W_S), then dried in an oven at 105 °C until constant weight was reached (W_i). The moisture content (MS) was calculated as follows [20]:

$$MS = \frac{W_s - W_i}{W_s} \times 100\% \qquad (1)$$

Where W_S is the initial film weight (g) and W_i is the final film dry weight (g).

Water solubility (WS) of film samples in water was determined based on a former method [9]. The conditioned film samples (4×4 cm^2) were weighed and dipped into 50 mL of distilled water with 0.1% (*w*/*v*) sodium azide as an antimicrobial agent. The samples were then shaken at a speed of 250 rpm for 24 h at 25 °C. After centrifugation at 8000 *g* for 10 min, samples were dried at 105 °C for 24 h to determine the weight of the remaining pieces of films (W_f). WS was calculated according to the following equation:

$$WS = \frac{W_i - W_f}{W_i} \times 100\% \qquad (2)$$

Where W_i is the final film dry weight (g) and W_i is the final dry weight of the remaining film (undissolved in water) weight (g). All tests were carried out in triplicate.

2.6 Water vapor permeability (WVP) and water contact angle

The WVP values of films were determined in triplicate (n=3) and measured gravimetrically according to the ASTM E96-05 Standard Method E96-00 [21]. A test cup (3 cm (depth) × 5 cm (diameter)) was filled with distilled water (15 mL) and the film (6 cm diameter) was placed over the opening. Then, the cups were placed in the desiccator at 25 °C and 50% relative humidity (RH).

Due to the difference in the water vapor pressure inside and outside the test cup, water was transferred through the film. The weights of the cups were recorded at 2 h intervals over a 12 h period. The measured WVP (g·mm/m^2·h·kPa) of the films was calculated as follows:

$$WVP = \frac{\Delta m \cdot d}{A \cdot t \cdot \Delta p} \quad (3)$$

where Δm is the weight change of the cup (g), D is the mean film thickness (mm), A is the area of exposed film (m^2), t is the time interval (2 h), and ΔP is the water vapor pressure difference (kPa) on both sides of the film. All tests were performed at least in triplicate.

Contact angles of the composite films were tested by means of an OCA20 contact angle analyzer (Dataphysics, Germany). Briefly, 5 μL per drop of distilled water was carefully deposited onto the surface of the film and angles were measured in five different regions of each surface and averaged. In addition, the image of the distilled water droplet was captured with a camera [9].

2.7 Opacity (OP)

To determine the opacity of the film, the ultraviolet spectrophotometer (Genesys 10S UV-VIS, Thermo Scientific, Thermo Fisher Scientific, USA) was used to measure the transmittance of the composite film at 350 nm to 800 nm. Meanwhile, absorbance of the film sample at 600 nm was used to calculate the opacity of the thin film. Each sample was repeated three times and the calculation formula was as follows:

$$OP = \frac{A_{600}}{d} \quad (4)$$

where OP is opacity, A_{600} is the absorbance value at 600 nm; D is the film thickness (mm). The higher value of OP indicates higher opacity and low degree of transparency [22].

2.8 Film morphology and color

After the films were dried, the prepared film was cut into 4×4 cm^2 size and conditioned at 50 ± 5% RH (25 °C, 48 h), the visual aspect of film samples was examined using a digital camera

177 (Fujifilm Finepix S4900; acquired from Fujifilm Thailand Co. Ltd., Bangkok, Thailand).

178 A precision Colorimeter (Shang Guang WSC-S, Shanghai, China) was used to determine color
179 attributes of the film and expressed as L*, a*, and b*. L* (brightness), a* (redness -greenness), b*
180 (yellowness-blueness) values were recorded. The whiteness (*W*) value was calculated using the
181 following equation [23] :

182 $$W = 100 - \sqrt{(100 - L^{*})^{2} + a^{*2} + b^{*2}} \qquad (5)$$

183 **2.9 Thermogravimetric analysis (TGA)**

184 TGA of the samples was performed by a thermogravimetric analyzer (PYRIS 1, Perkin-Elmer,
185 Waltham, Mass, USA) [24]. Each film sample (3-5 mg) was sealed in an aluminum plate and heated
186 from 30 °C to 600 °C at a heating rate of 10 °C/min in a nitrogen atmosphere (20 ml/min).

187 **2.10 X-ray diffraction (XRD)**

188 XRD was used to examine the crystallinity of MP-based composite films according to a former
189 method [25] with few modifications. All specimens were examined with a D8 Advance XRD
190 (Bruker, Germany) at room temperature and a scan angle from 5-80° with a step size of 0.02° 2θ
191 intervals using Ni-filtered K_{α} Cu X-ray radiation (wavelength of X-ray was 1.54 Å).

192 **2.11 Scanning electron microscopy (SEM)**

193 SEM was used to capture the image of the surface and cross-section of films (JSM-6390LV,
194 JEOL, Tokyo, Japan). The films (0.5 cm × 0.5 cm) were fixed on the bronze stub using double-sided
195 tape and were sputtered with gold using Sputter Coater SCD 005 (BAL-TEC AG, Balzers,
196 Liechtenstein). The voltage and the magnification used were 15 kV and 5000×magnification,
197 respectively [26].

198 **2.12 Atomic force microscopy (AFM)**

The surface topography of the prepared films was determined using AFM (MFP-3D, Asylum Research, USA) operated in intermittent contact/tapping mode [27]. The images were collected at a fixed scan rate of 0.5 Hz. The sampling rate was 512 lines. The morphology and the roughness data were processed using MF3D software (version 111111 + 1219).

2.13 Antioxidant activity

The antioxidant activity of the different composite films was assessed using DPPH (2,2-diphenyl-1-picrylhydrazyl) free radical scavenging assay according to the method described by Siripatrawan et al. with slight modification [28]. Film samples (10 mg) were added to 10 mL methanol. After they had completely dissolved, the film samples were oscillated at 25℃ for 2h. Then, 500 μL extraction of the composite film was mixed uniformly with 4.0 mL 150 μmol/L DPPH, and incubated in the dark for 30 min. The absorbance of the solution was measured at 517 nm, the percentage of DPPH free radical scavenging activity was calculated according to the following equation:

$$\text{DPPH scavenging Activity}(\%) = \frac{A_b - A_f}{A_b} \times 100 \qquad (6)$$

Where A_b is the absorbance of the control and A_f is the absorbance of the film sample.

2.14. Effect of different composite films on fish meat

2.14.1. Preparation of fish meat wrapped with films

Samples of fish meat (approximately 4×4 cm) were randomly divided into five groups. Five different kinds of films (Control, PVC, FMP/CS, FMP/CS/RE (0.1%) and FMP/CS/RE (0.2%)) prepared as described above were used to wrap fish meat samples. Samples without packaging were regarded as the control group. All samples were kept at 4 °C for 10 days and taken out for quality measurement on day 0, 2, 4, 6, 8 and 10.

221 **2.14.2 Thiobarbituric acid reactive substances (TBARS) and pH analysis**

222 TBARS were measured according to a former method [29]. Minced fish muscle (~5.00 *g*) was
223 homogenized (IKA Ultra-Turrax T18 Basic, Staufen, Germany) with 25 mL 7.5% (*w*/*v*)
224 trichloroacetic acid (containing 0.1% EDTA) for 1 min at 3000 rpm, then centrifuged (Fitchell SF-
225 TDL-5A, Shanghai, China) at a speed of 4000 *g* for 5 min. The supernatant (~5.0 mL) was mixed
226 with TBA (20 mM, 5 mL) solution; the mixture was incubated in a water bath at 100 °C for 30 min
227 and cooled with flowing water. The absorbance was measured with ultraviolet-visible
228 spectrophotometer (UV-VIS) at 532 nm (UNIC UV-2600 UV-Vis, Shanghai, China). The standard
229 curve was prepared using 1, 1, 3, 3-tetraethoxypropane. The results were expressed as milligrams
230 of malondialdehyde (MDA)/kg of fish sample. For measuring pH, ~3.0 g of the samples were
231 homogenized in 27.0 ml distilled water for about 30.0 min and centrifuged at a speed of 8000 g for
232 10.0 min. Then, pH was evaluated by placing the pH electrode in the samples.

233 **2.14.3 Free amino acid (FAA) and total volatile basic nitrogen (TVB-N)**

234 The content of FAA was determined by titration [30]. The minced fish sample (~5.00 *g*) was
235 homogenized with 15.0 ml ether-ethanol solution (2:1, *v*/*v*) at 3000 *g* for 1-2 min, then centrifuged
236 at a speed of 4000 *g* for 5.0 min and the supernatant collected. The same procedure was repeated
237 once as described above. The supernatant (~10.0 mL) was drawn off into an erlenmeyer flask, using
238 1% phenolphthalein as an indicator; the mixture was titrated with potassium hydroxide solution
239 (0.05 M). The FAA content was calculated and expressed as FAA in 100 *g* fish muscle sample.

240 The homogenized fish sample (~5.00 *g*) was extracted with 50 mL of deionized water for 30
241 min. After filtration, 5.0 mL filtrate and 10.0 mL flushing deionized water were mixed with 5.0 mL
242 of 0.1% (*w*/*v*) MgO. Then it was transferred to a 750 mL digestion tube. The tube was then installed

into an auto Kjeldahl nitrogen analysis system (FOSS Kjeltec 8400, Hilleroed, Denmark) for TVB-N measurement [31]. The TVB-N content was calculated and expressed as mg/100 *g* sample. The experiments were repeated in triplicate.

2.15 Statistical analysis

Results were analyzed using the statistical software SPSS 23.0 (SPSS Inc., Chicago, Illinois, USA). Data are presented as mean ± SD (standard deviation). Turkey test was used to determine the significant differences of the results ($p \leq 0.05$). All the tests in this study were carried out in triplicates, unless otherwise specified.

3. Results and discussion

3.1 Mechanical behavior analysis of the composite film

TS and EB of the composite films were used to assess the capability of the film's mechanical resistance to break and the stretching degree, respectively [32]. Generally, the mechanical behavior of a composite film changes with the corresponding composition variation. The TS and EB values of the composite film affected by different concentrations of RE are illustrated in Fig. 1. Results indicate that the addition of RE to FMP/CS films could significantly improve the TS of films, especially when the RE content was 0.05%. However, the TS of the FMP/CS/RE film showed a decreasing trend by increasing RE% to ratios higher than 0.05%. This may be due to the hydrophobic interaction formation between the benzene ring and carbonyl group which exist in RE and the hydrophobic regions of the myofibrillary protein. Nevertheless, EB of FMP/CS/RE films were reduced compared to the control. There are two possible explanations for this result. Firstly, the hydroxyl and carboxyl groups in RE bound with amino groups in the FMP which formed the

compact protein-phenolic network structure. The tight network structure leads to reduced film flexibility of the FMP/CS/RE films. Secondly, the enhanced intermolecular forces between RE and MP led to the destruction of the mobility of the film's molecular chains and decrease in flexibility of the film which contributed to the lowering of EB values of the composite film.

3.2 Physical characteristics of different composite films

The thickness, water content, solubility and WVP of the composite films are presented in Fig. 2. With the increase in RE contents, the thickness of the composite film gradually increased from 69.67 to 78.22 μm. The reason could be that the addition of RE increased the dry matter/film-forming substance content of the FMP/CS composite film. Furthermore, the increase in thickness of the composite films, might be related to the structure changes of the FMP/CS film with the addition of RE. This phenomenon is consistent with the results of Li et al. [33], namely the interaction between hydroxyl in polyphenol and glycerol and the film-forming matrix may have changed the structure of the film to some extent, thereby causing the thickness of the film to increase.

Compared with the control group, with the increase in content of RE, the water content of the composite film was significantly increased ($p < 0.05$). The reason could be that the presence of phenolic compounds led to the hydrophilic functional groups (−OH, NH_2 and −COOH) of the film to increase and strengthen the interaction (hydrogen bond) of water molecules [34]. In this study, the water solubility of the FMP/CS/RE composite film was higher than that in the control group, mainly due to the hydrophilicity of RE which was stronger than both the FMP and CS. The water solubility of the film in the groups containing RE was higher than that in the control group, arguably because the hydrophilicity of the RE was stronger than that of chitosan molecules and proteins, which is consistent with the results of Ashrafi et al. [35].

287 Generally, the WVP depends on the ratio of hydrophilic to hydrophobic components in the film
288 [36]. When RE was added, the values of WVP of composite films were higher than that of the
289 control. Basically, the trend of WVP of film kept rising as the RE concentration increased. This may
290 be caused by the existence of RE which reduced the crystallinity of the film and increased the
291 content of hydrophilic components within the film network structure which led the value of WVP
292 to increase. Binding of hydrophilic rosemary with macromolecular chains in film forming
293 components has been found to promote WVP in film substrates [37].

294 **3.2 Water contact angle (WCA)**

295 The hydrophilic and hydrophobic degree of the composite film surface were evaluated by
296 measuring the water contact angle between the film surface and water droplets [38]. The contact
297 angle of composite films is presented in Fig. 3. Essentially, the water contact angles of all groups
298 are less than 90°, indicating that the surfaces of all composite films are hydrophilic. The water
299 contact angle of the FMP/CS composite film was the largest and the WCA of the composite
300 membrane decreased following the increased content of RE. This means that the addition of RE
301 made the surface of the composite film more hydrophilic due to the hydrophilic nature of RE. This
302 outcome is also in agreement with the result of increased WVP and consistent to those obtained
303 from the bilayer edible films made by hydrophobic ethyl cellulose and hydrophilic carboxymethyl
304 chitosan hydrogel [39]. Nonetheless, these results are distinct from findings on films based on
305 cassava starch films modified with polyphenols-rich RE [40]. This different behavior can be
306 explained on the basis that hydrophobicity of the main bioactive compounds is isolated from the
307 aqueous RE (such as rosmaniric acid and carnosic acid). A comparison of these two compounds
308 shows that, carnosic acid is more hydrophobic with two OH groups and a COOH group, whereas

309 rosmaniric acid has four OH groups and a COOH group. In this sense, the increase in the film
310 surface hydrophobicity could be attributed to the amounts of carnosic acid, which could migrate to
311 the film surface during the drying process. The purity of rosmaniric acid used in our study was very
312 high, it is about 80%, but the RE used in that reference were extracted from dried and milled
313 rosemary leaves only. Thus, the purity of rosmaniric acid is far below that used in this study, as it is
314 only about 2.6% after estimation.

315 **3.3 Appearance and color analysis**

316 The color of the film affects the appearance of the food. Thus, it is an important parameter for
317 the preparation process of the edible film. Plant extracts can usually change the color of the film.
318 Numerous studies have reported that the degree of color change by the addition of plant extracts
319 depends on the species and the concentration of the plant extract [41]. Usually, the color difference
320 is determined by three parameters, such as L, a and b. The values of these three parameters are
321 collected in Table 1. When RE was added, all color parameters of the film showed significant
322 differences. As the rosemary concentration increased, a decrease in the L value indicated that the
323 film became darker and an increase in the a and b values suggests that the color of the film tended
324 to be redder and yellower. In addition, an increase in ΔE was observed. The above data shows that
325 as the concentration of rosemary increased, the film became darker, yellower and slightly reddish.
326 The oxidation of phenolic compounds in rosemary can change the color and as the temperature
327 increases, the color of phenolic compounds becomes darker. The reason may be due to two aspects.
328 On the one hand, Maillard reaction may have occurred between the fish protein and carbohydrates,
329 while on the other hand, yellow pigments could have formed in acidic conditions causing the degree
330 of color change to be affected by processing conditions and moisture content [42].

3.4 Light transmittance and opacity

In general, plant extracts can cause an increase in the opacity of composite films due to their color [36]. The effect of adding RE onto the transmittance and opacity of the FMP/CS film is shown in Table 2. It can be seen that the composite film with RE has lower light transmittance and higher opacity when compared with the control. Moreover, the opacity of the composite film was positively correlated with the RE concentration. With the increase of RE concentration, the opacity of FMP/CS/RE films displayed excellent visible light blocking performance. Wen et al. also found that light transmittance of polyvinyl alcohol composite film decreased with the increase in green tea extract [43]. The low light transmittance and high opacity can effectively prevent the decomposition of photosensitive ingredients in foods, which is extremely important for food packaging and this result is also consistent with the color measurement of composite films. The decrease in transparency and increase in opacity may be due to the presence of coloring RE which contributes significantly to reducing of the transmission of light [44]. In addition, the light selective absorption of polyphenol compounds exist in the extracts at low wavelengths which expresses a reddish color in the films, thus decreasing the light transmittance and opacity [45].

3.5 TGA analysis

The decomposition pattern and the thermal stability of different films were evaluated utilizing TGA analysis, which are presented in Fig. 4. Following the water desorption, a three-step decomposition curve was observed. The first stage (30-150°C, weight loss: 20-25 %) was possibly due to loss of free water, bound water and acetic acid which remained in the film [46]. The second stage (150-300 °C, weight loss: 25-60%) could mainly be attributed to thermal degradation of the glycerol rich phase, FMP and skeleton protein that exist in film substrates. Compared with the

FMP/CS composite film, the weight loss of the composite film was reduced by 5-15 % when 0.05-0.2 % RE was added. The reason may be that the addition of RE enhanced the thermal stability of the composite film, thus, the degradation temperature was increased. The trend of increasing decomposition temperature indicates that there are stronger interactions between RE and FMP/CS film matrix [47]. The existence of polyphenol- cross-linked FMP networks led to the higher thermal degradation temperature [8]. Furthermore, the higher concentration of RE (0.1-0.2%) increased the hydrophilicity of the MP/CS/RE composite film, which could lead to the increase of water content in the film, hence, the thermal stability was lower than that of RE content (0.05%). The thermal decomposition of the third stage which occurred at 300-600 °C could be attributed to the further degradation and carbonization of the remaining products after thermal degradation during the first two stages. This could explain the low content of flame retardant material in the prepared composite film [48].

3.6 XRD analysis

An amorphous structure predominates in composite films as demonstrated by the X-ray diffraction pattern in Fig. 5. The composite films of all samples show two specific peaks at 2θ of 8° and 20°. The same two peaks appeared in XRD spectrums of a series of chitosan/zein blend films with different proportions [47]. Owing to the amorphous crystal structure that exist in the composite film, there are no high-intensity diffraction peak which appeared in the spectrum. The presence of RE with different percentages in the FMP/CS polymer substrate led to the intensity of diffraction peaks at 2θ to increase. When the concentration of RE was 0.2%, the intensity of the diffraction peaks at 2θ significantly increased, which indicates that the compatibility of FMP, CS and RE was slightly decreased [49]. The result is confirmed by SEM and AFM analysis.

3.7 Composite film morphology observed by SEM

SEM morphology was used to explore the uniformity and network structure of the film forming matrix. The surface and cross-sectional SEM micrographs of FMP/CS films incorporated with different concentrations of RE are illustrated in Fig. 6. It can be observed that there are some differences in the surface and cross-section structure morphology between the FMP/CS film and FMP/CS/RE films. The surface of the FMP/CS composite film (Fig. 6A) is uniform and smooth, without holes, pores or cracks in the cross-sectional view, which indicates that the FMP and CS have good compatibility and film-forming properties. The addition of RE had an obvious effect on the surface of the FMP/CS film. When the concentration of RE was 0.05%, the surface of the composite film remained smooth, and there were no obvious holes in the cross section, indicating that the low concentration of RE was well-distributed into the film matrix with strong interactions and all the film-forming matrix demonstrated better compatibility (Fig. 6B). With the increase in concentration of RE, the surface of the composite film exhibited "protrusions", which could be related to the interaction between RE and the film-forming matrix. The excessive amount of RE (0.2%) destroyed the internal structure and weakened the intermolecular forces between polymer chains, making the film relatively loose (Fig. 6C and 5D). Furthermore, more pores or cavities appeared in the cross-section structure morphology of FMP/CS/RE films with excessive RE%, which resulted in the aggregation and non-uniform dispersion of the RE in the film forming matrix, and led to irregularities [50]. Similar results are reported were rougher film surface was obtained in alginate composite films with the addition of green tea extract and a grape seed extract [45]. The holes observed in the cross-section structure of the film are enlarged, which somewhat just explains the increase in the WVP of the film. In addition, when comparing the scale of the cross-sectional view

(multiplier: 1000), it can be seen that the higher the concentration of RE is, the thicker of composite film, which is consistent with the results of thickness.

3.8 AFM image

The morphology and roughness of FMP/CS composite film affected by different concentration of RE treated composite films is shown in Fig. 7. It can be seen very clearly that the surface of the FMP/CS composite film is overall flat with slight concaves. There are a few light spots on the 3D image, which can be explained as the product generation of the interaction between FMP and CS. When 0.05% concentration of RE was added, the composite film displayed a smooth surface compared with the control film, indicating that a good distribution of RE in the blend of FMP/CS matrix was attained due to the cross-linking of FMP and CS, which is in agreement with the results obtained by SEM. However, as soon as the concentration of RE reached 0.10–0.20%, the surface roughness of the composite film increased and some of "gulls" emerged. This result may be due to the molecular interaction between the composite FMP/CS film and RE, which is in agreement with the previous report that reported that the surface roughness of films was increased because of the interaction between film-forming substances[51]. An adverse result was found in study on edible film based on potato starch, olive oil and zein nanoparticles[27].

3.9 Antioxidant activity

The addition of antioxidants can change the color of the film and inhibit the oxidation of lipid components, thus extending the shelf life of packaged products. The major polyphenolic compound in RE is rosmarinic acid, which is known for its oxidation resistance, anti-inflammatory, antibacterial and other properties[52]. Therefore, adding RE to the composite film can increase the antioxidant capacity of the film to some extent. DPPH radical scavenging assay has been widely

used to test the antioxidant activity of polyphenolic compounds. Antioxidant activity expressed in terms of DPPH radical scavenging activity of FMP/CS films adding different concentrations of RE is shown in Fig.8. The DPPH radical scavenging ability of the control FMP/CS film was low, while the antioxidant activity capacity of the FMP/CS/RE composite film increased with the level of RE. The maximum antioxidant activity was observed in film containing RE concentration of 0.20%. This could be due to the antioxidant activity of the composition of film-forming materials, such as MP, CS and RE. This phenomenon is consistent with former results [53] - the antioxidant activity of the MP film without the addition of catechin-Kradon extract had the lowest value. Furthermore, it fundamentally shows a positive correlation between the amount of polyphenol and antioxidant capacity, which is identical with the conclusion of Gomez-Estaca et al [54]. Rosemary and oregano extracts were added into tuna-skin and bovine-hide gelatin based films, the strength of antioxidant activity of the gelatine films attributed to the content of phenolic compounds of additives.

3.10 Quality changes in fish fillets during storage

3.10.1 Thiobarbituric acid reactive substances (TBARS)

TBARS is an indicator of the degree of lipid oxidation, which is induced by the accumulation of lipid peroxides and the corresponding secondary metabolites [55]. As shown in Fig. 9A, the initial TBARS was 0.29 mg MDA/kg per sample and the TBARS of each group did not indicate any significant difference ($p>0.05$). From the six days of storage, the TBARS value of RE groups were significantly lower than that of the control. On account of the extension of the storage periods, peroxides like malondialdehyde (MDA) are produced and increased with the oxidation of unsaturated fatty acids [56]. During the late storage period (10 days), the TBARS (1.24 mg MDA/kg sample) of the control was significantly higher than that of the other groups. This result is consistent

441 with RE or other phenolic compounds that have strong free radical scavenging capability, which can
442 decrease the degree of lipid oxidation [57]. Furthermore, the content of phenolic compound of the
443 film-forming materials restricts the lipid oxidation and decreases the TBARS values.

444 **3.10.2 pH**

445 The pH of fish is an indicator reflecting the freshness of the fish quality after death. The change
446 in pH of grass carp flesh during cold storage is illustrated in Fig. 9B. It can be seen that the pH of
447 all groups showed a similar trend -a decreasing and then an increasing trend. During the early stage
448 of refrigeration (0-4 days), the pH values were decreased which could be due to the glycolysis of
449 grass carp flesh that led to the accumulation of lactic acid and the degradation of adenosine
450 triphosphate (ATP) to release inorganic phosphate. With the extension of refrigeration time (4-10
451 days), the autolysis of fish protein and the formation of basic compounds (ammonia and trim-
452 ethylamine) caused by the action of microorganisms has been shown to lead to a gradual increase
453 in the pH value [58]. During the storage period, compared with the control group, the pH value of
454 both the PVC film and FMP/CS composite film groups increased slowly, but the pH of the
455 FMP/CS/RE composite film exhibited the slowest increase among all sample groups. The pH
456 increase rate of the group was opposite to the concentration in RE, which could be due to certain
457 inhibitory effects of RE on the microorganisms of fish meat. This is consistent with the study of the
458 pH value of mud shrimp (*Solenocera melantho*) treated with RE which was significantly lower than
459 that of the control during the frozen storage [11].

460 **3.10.3 Changes in FAA in fish fillets**

461 The content of FAA in fish fillets is a common indicator for evaluating the spoilage of aquatic
462 products. The changes in FAA detected in grass carp flesh wrapped with different composite

463 film/coating are illustrated (Fig. 9C). Firstly, it can be seen that the content of FAA of grass carp
464 flakes increased with the extension of storage time, indicating that the lipids in fish flesh are
465 continuously hydrolyzed during cold storage. In this study, the sample wrapped with the films
466 inhibited lipid hydrolysis to some extent. The speed of FAA production rate for fish flesh under
467 different treatments were as following: the control group > the PVC film group > the FMP/CS group >
468 the FMP/CS/RE (0.1%) > the FMP/CS/RE (0.2%). The major factor affecting the lipid hydrolysis
469 during the fish late storage period is microbial activities [59]. Therefore, the results indicate that RE
470 could affect microbial activities in the fish muscle during the cold storage of grass carp flakes.

471 **3.10.4 Volatile base nitrogen (TVB-N)**

472 The value of TVB-N is an intuitive reflective indicator of food spoilage. TVB-N is positively
473 correlated with the activity of endogenous enzymes in fish and the growth of microorganisms [60].
474 The changes in TVB-N detected in grass carp flakes during cold storage are shown in Fig. 9D.
475 Compared with the TVB-N value of grass carp meat on 0 day (9 mg/100g), the TVB-N values of all
476 groups were increased. After the 4^{th} day, the TVB-N values of FMP/CS/RE groups were
477 significantly lower than those of the control and the PVC film groups ($p>0.05$). The result illustrates
478 that the RE composite film could extend the shelf life of grass carp flakes and is more effective
479 compared to the plastic fresh-keeping film. This is consistent with the finding of edible coating
480 enriched with RE that enhanced the oxidative and microbial stability of smoked eel fillets [15].

481 **4. Conclusion**

482 In the present study, composite films based on FMP/CS incorporated with RE were developed.
483 The composite films showed considerable mechanical properties, acceptable moisture barrier
484 capability as well as good compatibility which are supported by results of SEM and AFM images.
485 Moreover, the composite films were applied in order to preserve grass carp fillets. Results indicate

that FMP/CS/RE (0.20%) composite films possessed the best protective effect on fish muscle, maintaining a low pH value and FAA values. The changes in TVB-N and TBARS show that the degree of lipid oxidation of fish muscle decreased during the seven days refrigerated storage. It was therefore suggested that the prepared composite film FMP/CS/RE could have potential for improving the quality and shelf life of fish muscle.

Acknowledgments

This work was funded by the Fundamental Research Funds for the Central Universities of China (No. 2662019PY031) and the National Natural Science Foundation of China (No. 31772047).

References

[1] W. Theerawitayaart, T. Prodpran, S. Benjakul, K. Nilsuwan, K. de la Caba, Storage stability of fish gelatin films by molecular modification or direct incorporation of oxidized linoleic acid: Comparative studies, Food Hydrocolloids, 113 (2020) 106481.

[2] C. Wang, T. Chang, S. Dong, D. Zhang, C. Ma, S. Chen, H. Li, Biopolymer films based on chitosan/potato protein/linseed oil/ZnO NPs to maintain the storage quality of raw meat, Food Chemistry, 332 (2020) 127375.

[3] J. Park, J. Nam, H. Yun, H.-J. Jin, H.W. Kwak, Aquatic polymer-based edible films of fish gelatin crosslinked with alginate dialdehyde having enhanced physicochemical properties, Carbohydrate Polymers, 254 (2021) 117317.

[4] H. Wang, F. Ding, L. Ma, Y. Zhang, Edible films from chitosan-gelatin: Physical properties and food packaging application, Food Bioscience, 40 (2021) 100871.

[5] S.A.A. Mohamed, M. El-Sakhawy, M.A.-M. El-Sakhawy, Polysaccharides, Protein and Lipid -Based Natural Edible Films in Food Packaging: A Review, Carbohydrate Polymers, 238 (2020) 116178.

[6] L. Dou, B. Li, K. Zhang, X. Chu, H. Hou, Physical properties and antioxidant activity of gelatin-sodium alginate edible films with tea polyphenols, International Journal of Biological Macromolecules, 118 (2018) 1377-1383.

[7] X. Nie, Y. Gong, N. Wang, X. Meng, Preparation and characterization of edible myofibrillar protein-based film incorporated with grape seed procyanidins and green tea polyphenol, LWT - Food Science and Technology, 64 (2015) 1042-1046.

[8] T. Prodpran, S. Benjakul, S. Phatcharat, Effect of phenolic compounds on protein cross-linking and properties of film from fish myofibrillar protein, International Journal of Biological Macromolecules, 51 (2012) 774-782.

[9] B. Shabanpour, M. Kazemi, S.M. Ojagh, P. Pourashouri, Bacterial cellulose nanofibers as reinforce in edible fish myofibrillar protein nanocomposite films, International Journal of Biological Macromolecules, 117 (2018) 742-751.

[10] J.T.S. Batista, C.S. Araújo, M.R.S. Peixoto Joele, J.O.C. Silva, L.F.H. Lourenço, Study of the effect of

the chitosan use on the properties of biodegradable films of myofibrillar proteins of fish residues using response surface methodology, Food Packaging and Shelf Life, 20 (2019) 100306.
[11] J. Shi, Y. Lei, H. Shen, H. Hong, X. Yu, B. Zhu, Y. Luo, Effect of glazing and rosemary (Rosmarinus officinalis) extract on preservation of mud shrimp (Solenocera melantho) during frozen storage, Food Chemistry, 272 (2019) 604-612.
[12] V.A. Tironi, M.C. Tomás, M.C. Añón, Quality loss during the frozen storage of sea salmon (Pseudopercis semifasciata). Effect of rosemary (Rosmarinus officinalis L.) extract, LWT - Food Science and Technology, 43 (2010) 263-272.
[13] D. Georgantelis, G. Blekas, P. Katikou, I. Ambrosiadis, D.J. Fletouris, Effect of rosemary extract, chitosan and α-tocopherol on lipid oxidation and colour stability during frozen storage of beef burgers, Meat Science, 75 (2007) 256-264.
[14] S. Jancikova, E. Jamróz, P. Kulawik, J. Tkaczewska, D. Dordevic, Furcellaran/gelatin hydrolysate/rosemary extract composite films as active and intelligent packaging materials, International Journal of Biological Macromolecules, 131 (2019) 19-28.
[15] E. Choulitoudi, S. Ganiari, T. Tsironi, A. Ntzimani, D. Tsimogiannis, P. Taoukis, V. Oreopoulou, Edible coating enriched with rosemary extracts to enhance oxidative and microbial stability of smoked eel fillets, Food Packaging and Shelf Life, 12 (2017) 107-113.
[16] W. Xie, Y. Huang, Y. Xiang, S. Xiong, A. Manyande, H. Du, Insights into the Binding Mechanism of Polyphenols and Fish Myofibrillar Proteins Explored Using Multi-spectroscopic Methods, Food and Bioprocess Technology, 13 (2020) 797-806.
[17] O.H. Lowry, N.J. Rosebrough, A.L. Farr, R.J. Randall, Protein measurement with the Folin phenol reagent, Journal of Biological Chemistry, 193 (1951) 265-275.
[18] S. Nuanmano, T. Prodpran, S. Benjakul, Potential use of gelatin hydrolysate as plasticizer in fish myofibrillar protein film, Food Hydrocolloids, 47 (2015) 61-68.
[19] C. Zhang, Z. Wang, Y. Li, Y. Yang, X. Ju, R. He, The preparation and physiochemical characterization of rapeseed protein hydrolysate-chitosan composite films, Food Chemistry, 272 (2019) 694-701.
[20] D.C. Da Silva, I.A. Lopes, L.J.S. Da Silva, M.F. Lima, A.K.D. Barros Filho, H.A. Villa-Vélez, A.A. Santana, Physical properties of films based on pectin and babassu coconut mesocarp, International Journal of Biological Macromolecules, 130 (2019) 419-428.
[21] ASTM, in, West Conshohocken, PA, 2015.
[22] C. Wang, T. Chang, S. Dong, D. Zhang, H. Li, Biopolymer films based on chitosan/potato protein/linseed oil/ZnO NPs to maintain the storage quality of raw meat, Food Chemistry, 332 (2020) 127375.
[23] J.W. PARK, Surimi Gel Colors as Affected by Moisture Content and Physical Conditions, Journal of Food Science, 60 (1995) 15-18.
[24] L. Zhang, Z. Zhang, Y. Chen, X. Ma, M. Xia, Chitosan and procyanidin composite films with high antioxidant activity and pH responsivity for cheese packaging, Food Chemistry, 338 (2021) 128013.
[25] L. Wang, J. Ding, Y. Fang, X. Pan, F. Fan, P. Li, Q. Hu, Effect of ultrasonic power on properties of edible composite films based on rice protein hydrolysates and chitosan, Ultrasonics Sonochemistry, 65 (2020) 105049.
[26] K.S. Silva, T.M.R. Fonseca, L.R. Amado, M.A. Mauro, Physicochemical and microstructural properties of whey protein isolate-based films with addition of pectin, Food Packaging and Shelf Life, 16 (2018) 122-128.
[27] R. Farajpour, Z. Emam Djomeh, S. Moeini, H. Tavakolipour, S. Safayan, Structural and physico-

566 mechanical properties of potato starch-olive oil edible films reinforced with zein nanoparticles,
567 International Journal of Biological Macromolecules, 149 (2020) 941-950.
568 [28] U. Siripatrawan, W. Vitchayakitti, Improving functional properties of chitosan films as active food
569 packaging by incorporating with propolis, Food Hydrocolloids, 61 (2016) 695-702.
570 [29] Q. Cao, H. Du, Y. Huang, Y. Hu, A. Manyande, The inhibitory effect of chlorogenic acid on lipid
571 oxidation of grass carp (Ctenopharyngodon idellus) during chilled storage, Food and Bioprocess
572 Technology, 12 (2019) 2050-2061.
573 [30] J.J. Cordoba, T. Antequera, C. Garcia, J. Ventanas, M.A. Asensio, Evolution of free amino acids and
574 amines during ripening of Iberian cured ham, Journal of Agricultural & Food Chemistry, 42 (1994) 2296-
575 2301.
576 [31] X. Zhao, J.e. Wu, L. Chen, H. Yang, Effect of vacuum impregnated fish gelatin and grape seed extract
577 on metabolite profiles of tilapia (Oreochromis niloticus) fillets during storage, Food Chemistry, 293
578 (2019) 418-428.
579 [32] M. Jahromi, M. Niakousari, M.T. Golmakani, M.A. Mohammadifar, Physicochemical and structural
580 characterization of sodium caseinate based film-forming solutions and edible films as affected by high
581 methoxyl pectin, International Journal of Biological Macromolecules, 165 (2020) 1949-1959.
582 [33] J.H. Li, J. Miao, J.L. Wu, S.F. Chen, Q.Q. Zhang, Preparation and characterization of active gelatin-
583 based films incorporated with natural antioxidants, Food Hydrocolloids, 37 (2014) 166-173.
584 [34] A. Aljawish, L. Muniglia, A. Klouj, J. Jasniewski, J. Scher, S. Desobry, Characterization of films based
585 on enzymatically modified chitosan derivatives with phenol compounds, Food Hydrocolloids, 60 (2016)
586 551-558.
587 [35] A. Ashrafi, M. Jokar, A. Mohammadi Nafchi, Preparation and characterization of biocomposite film
588 based on chitosan and kombucha tea as active food packaging, International Journal of Biological
589 Macromolecules, 108 (2018) 444-454.
590 [36] K. Norajit, K.M. Kim, G.H. Ryu, Comparative studies on the characterization and antioxidant
591 properties of biodegradable alginate films containing ginseng extract, Journal of Food Engineering, 98
592 (2010) 377-384.
593 [37] L. Sánchez-González, M. Cháfer, A. Chiralt, C. González-Martínez, Physical properties of edible
594 chitosan films containing bergamot essential oil and their inhibitory action on Penicillium italicum,
595 Carbohydrate Polymers, 82 (2010) 277-283.
596 [38] Y.-C. Yin, S.-W. Yin, X.-Q. Yang, C.-H. Tang, S.-H. Wen, Z. Chen, B.-j. Xiao, L.-Y. Wu, Surface modification
597 of sodium caseinate films by zein coatings, Food Hydrocolloids, 36 (2014) 1-8.
598 [39] P. Shao, W. Wu, H. Chen, P. Sun, H. Gao, Bilayer edible films with tunable humidity regulating
599 property for inhibiting browning of Agaricus bisporus, Food Research International, 138 (2020) 109795.
600 [40] D. Piñeros-Hernandez, C. Medina-Jaramillo, A. López-Córdoba, S. Goyanes, Edible cassava starch
601 films carrying rosemary antioxidant extracts for potential use as active food packaging, Food
602 Hydrocolloids, 63 (2017) 488-495.
603 [41] A. Silva-Weiss, M. Ihl, P.J.A. Sobral, M.C. Gómez-Guillén, V. Bifani, Natural Additives in Bioactive
604 Edible Films and Coatings: Functionality and Applications in Foods, Food Engineering Reviews, 5 (2013)
605 200-216.
606 [42] L. Zeng, M. Ma, C. Li, L. Luo, Stability of Tea Polyphenols Solution with Different pH at Different
607 Temperatures, International Journal of Food Properties, 20 (2017) 1-18.
608 [43] H. Wen, Y.I. Hsu, T.A. Asoh, H. Uyama, Antioxidant activity and physical properties of pH-sensitive
609 biocomposite using poly(vinyl alcohol) incorporated with green tea extract, Polymer Degradation and

610 Stability, 178 (2020) 109215.
611 [44] S. Munir, Y. Hu, Y. Liu, S. Xiong, Enhanced properties of silver carp surimi-based edible films
612 incorporated with pomegranate peel and grape seed extracts under acidic condition, Food Packaging
613 and Shelf Life, 19 (2019) 114-120.
614 [45] M.J. Fabra, I. Falcó, W. Randazzo, G. Sánchez, A. López-Rubio, Antiviral and antioxidant properties
615 of active alginate edible films containing phenolic extracts, Food Hydrocolloids, 81 (2018) 96-103.
616 [46] A. Sadeghi-Varkani, Z. Emam-Djomeh, G. Askari, Physicochemical and microstructural properties of
617 a novel edible film synthesized from Balangu seed mucilage, International Journal of Biological
618 Macromolecules, 108 (2018) 1110-1119.
619 [47] L. Zhang, Z. Liu, X. Wang, S. Dong, Y. Sun, Z. Zhao, The properties of chitosan/zein blend film and
620 effect of film on quality of mushroom (Agaricus bisporus), Postharvest Biology and Technology, 155
621 (2019) 47-56.
622 [48] M. Mujtaba, L. Akyuz, B. Koc, M. Kaya, S. Ilk, D. Cansaran-Duman, A.S. Martinez, Y.S. Cakmak, J.
623 Labidi, S. Boufi, Novel, multifunctional mucilage composite films incorporated with cellulose nanofibers,
624 Food Hydrocolloids, 89 (2019) 20-28.
625 [49] K. Wang, K. Wu, M. Xiao, Y. Kuang, H. Corke, X. Ni, F. Jiang, Structural characterization and properties
626 of konjac glucomannan and zein blend films, International Journal of Biological Macromolecules, 105
627 (2017) 1096-1104.
628 [50] Y. Lei, H. Wu, C. Jiao, Y. Jiang, R. Liu, D. Xiao, J. Lu, Z. Zhang, G. Shen, S. Li, Investigation of the
629 structural and physical properties, antioxidant and antimicrobial activity of pectin-konjac glucomannan
630 composite edible films incorporated with tea polyphenol, Food Hydrocolloids, 94 (2019) 128-135.
631 [51] Jiang, Fatang, Corke, Harold, Fang, Yapeng, Xuewen, Wan, Li, Xiao, Characterization of konjac
632 glucomannan-ethyl cellulose film formation via microscopy, International Journal of Biological
633 Macromolecules: Structure, Function and Interactions, 85 (2016) 434-441.
634 [52] D.C. Costa, H.S. Costa, T.G. Albuquerque, F. Ramos, M.C. Castilho, A. Sanches-Silva, Advances in
635 phenolic compounds analysis of aromatic plants and their potential applications, Trends in Food Science
636 & Technology, (2015) 336-354.
637 [53] P. Kaewprachu, N. Rungraeng, K. Osako, S. Rawdkuen, Properties of fish myofibrillar protein film
638 incorporated with catechin-Kradon extract, Food Packaging and Shelf Life, 13 (2017) 56-65.
639 [54] J. Gómez-Estaca, L. Bravo, M.C. Gómez-Guillén, A. Alemán, P. Montero, Antioxidant properties of
640 tuna-skin and bovine-hide gelatin films induced by the addition of oregano and rosemary extracts, Food
641 Chemistry, 112 (2009) 18-25.
642 [55] T. Le, K. Takahashi, E. Okazaki, K. Osako, Mitigation of lipid oxidation in tuna oil using gelatin pouches
643 derived from horse mackerel (Trachurus japonicus) scales and incorporating phenolic compounds, LWT,
644 128 (2020) 109533.
645 [56] L. Sun, J. Sun, P. Thavaraj, X. Yang, Y. Guo, Effects of thinned young apple polyphenols on the quality
646 of grass carp (Ctenopharyngodon idellus) surimi during cold storage, Food Chemistry, 224 (2017) 372-
647 381.
648 [57] U. Siripatrawan, B.R. Harte, Physical properties and antioxidant activity of an active film from
649 chitosan incorporated with green tea extract, Food Hydrocolloids, 24 (2010) 770-775.
650 [58] F. Farajzadeh, A. Motamedzadegan, S.-A. Shahidi, S. Hamzeh, The effect of chitosan-gelatin coating
651 on the quality of shrimp (Litopenaeus vannamei) under refrigerated condition, Food Control, 67 (2016)
652 163-170.
653 [59] L. Sun, J. Sun, D. Liu, M. Fu, X. Yang, Y. Guo, The preservative effects of chitosan film incorporated

654 with thinned young apple polyphenols on the quality of grass carp (Ctenopharyngodon idellus) fillets
655 during cold storage: Correlation between the preservative effects and the active properties of the film,
656 Food Packaging & Shelf Life, 17 (2018) 1-10.
657 [60] M.Y. Arancibia, M.E. López-Caballero, M.C. Gómez-Guillén, P. Montero, Chitosan coatings enriched
658 with active shrimp waste for shrimp preservation, Food Control, 54 (2015) 259-266.
659
660

661 **Table 1: Appearance and color parameters of different composite films.**

RE content (%)	Appearance	L*	a*	b*	ΔE
FMP/CS		93.31±0.64^{a}	1.33±0.17^{c}	9.00±1.32^{e}	8.68±1.34^{e}
FMP/CS/ RE (0.05%)		89.67±0.64^{b}	0.58±0.05^{b}	12.59±1.26^{d}	12.86±1.37^{d}
FMP/CS/RE (0.10%)		88.06±0.82^{c}	0.63±0.09^{b}	15.20±1.33^{c}	15.85±1.53^{c}
FMP/CS/RE (0.15%)		86.74±0.21^{d}	0.20±0.17^{a}	17.44±0.54^{b}	18.43±0.56^{b}
FMP/CS/RE (0.20%))		85.56±0.93^{e}	0.04±0.22^{a}	19.68±2.03^{a}	20.94±2.21^{a}

662 Note: Values are presented as mean ± standard error. Means in the same line with different

663 subscripts (a, b, c, d, e) are significantly different ($p<0.05$).

664

665 **Table 2: Light transmittance and transparency of composite films treated with different**

666 **concentrations of RE.**

RE（%，W/W）	Transmittance (%T) at wavelength（nm）						Opacity
	350	400	500	600	700	800	
0	47.1	56.77	64.34	72.34	73.21	73.78	2.1 ± 0.05^{e}
0.05%	0.063	46.28	50.31	63.85	64.34	64.75	3.16 ± 0.07^{d}
0.10%	0.046	42.43	48.32	58.73	59.25	60.02	3.50 ± 0.14^{c}
0.15%	0.022	39.35	44.76	49.37	50.23	51.05	5.01 ± 0.12^{b}
0.20%	0.002	34.25	37.46	40.14	41.05	41.94	5.75 ± 0.11^{a}

667 Note: Different superscripts a, b, c, d, e in each column indicate significant differences ($p<0.05$).

668 Values are given as mean ± SD from triplicate determinations.

669

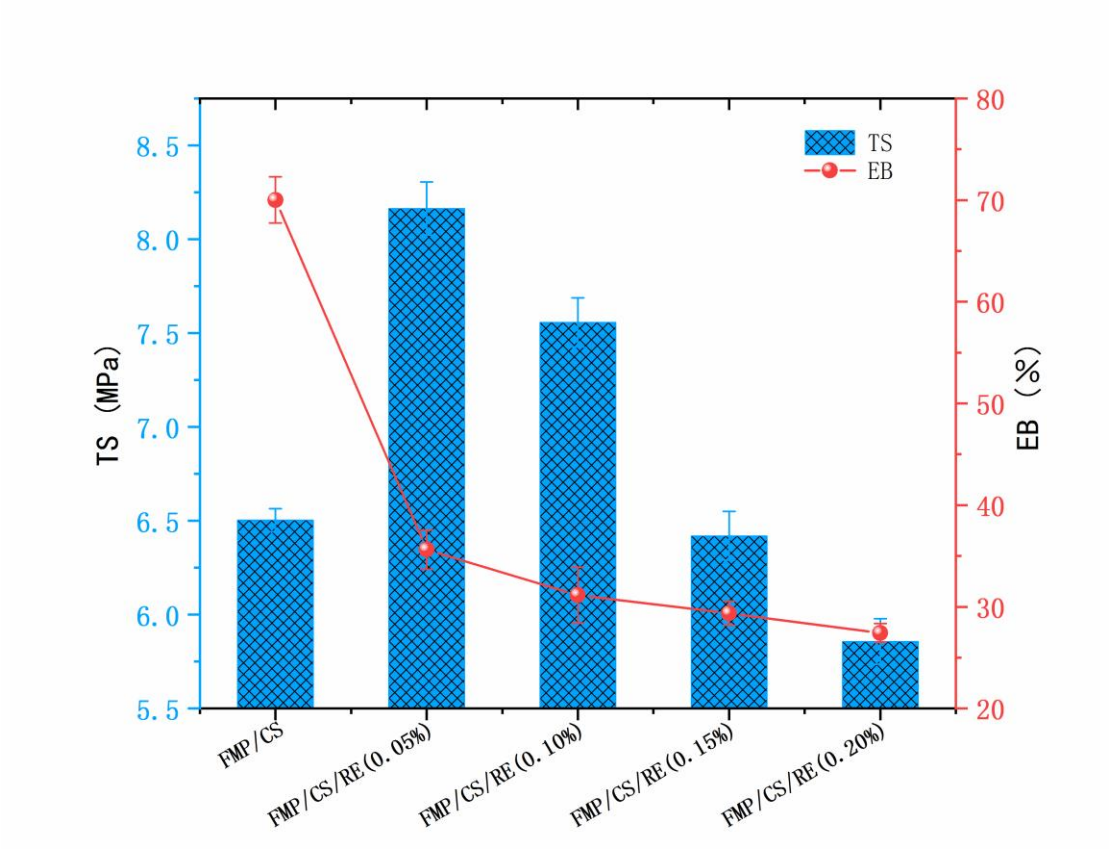

Fig. 1: The mechanical properties of different composite films

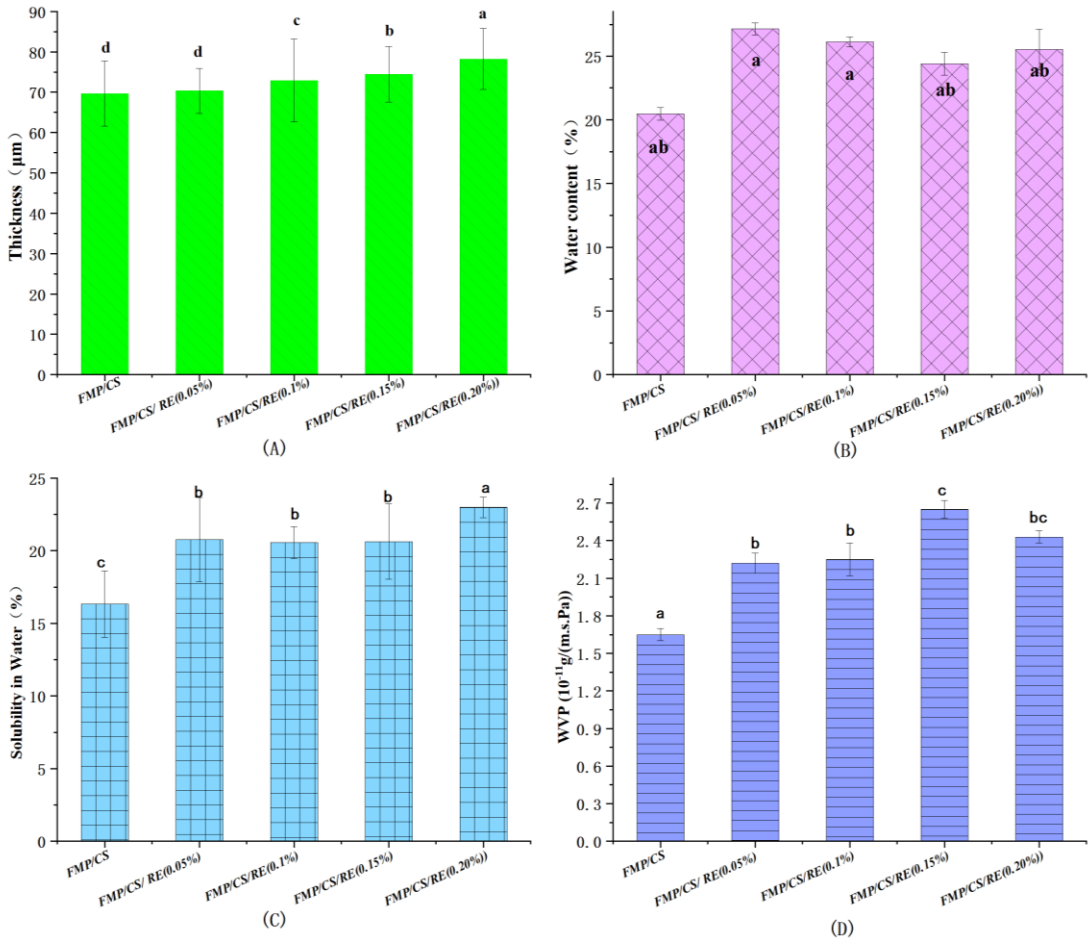

Fig. 2: Thickness, water content, solubility and water vapor permeability of different composite films. Note: The letters a, b, c, d (different letters in the same column) indicate significant differences (p<0.05).

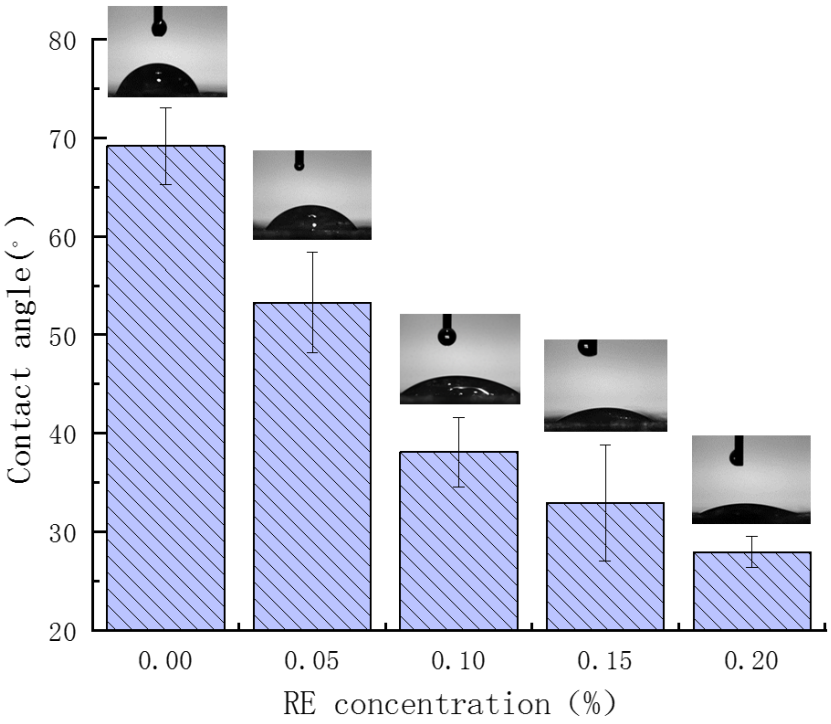

679
680
681 **Fig. 3: Water contact angle of the composite films.**
682
683

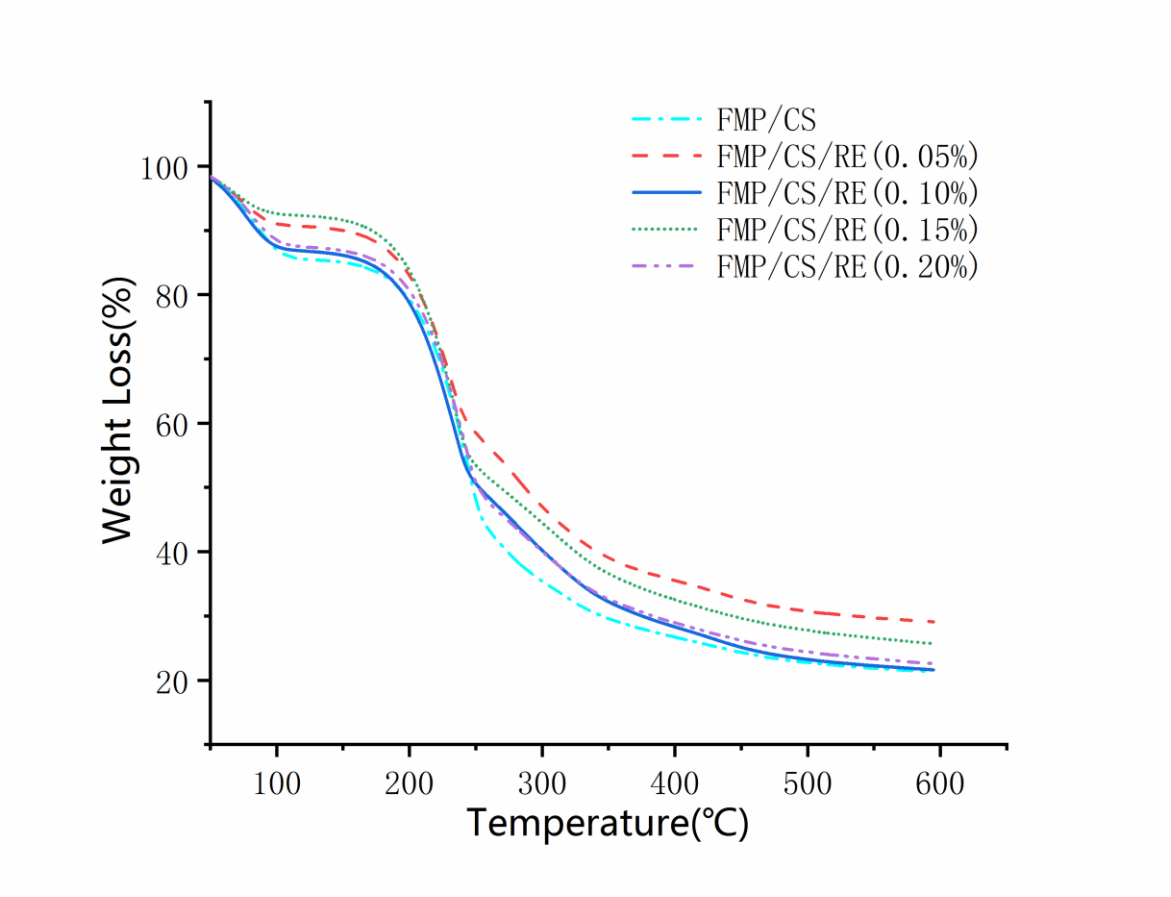

684

685 **Fig. 4: TGA curves of different composite films**

686

687

688

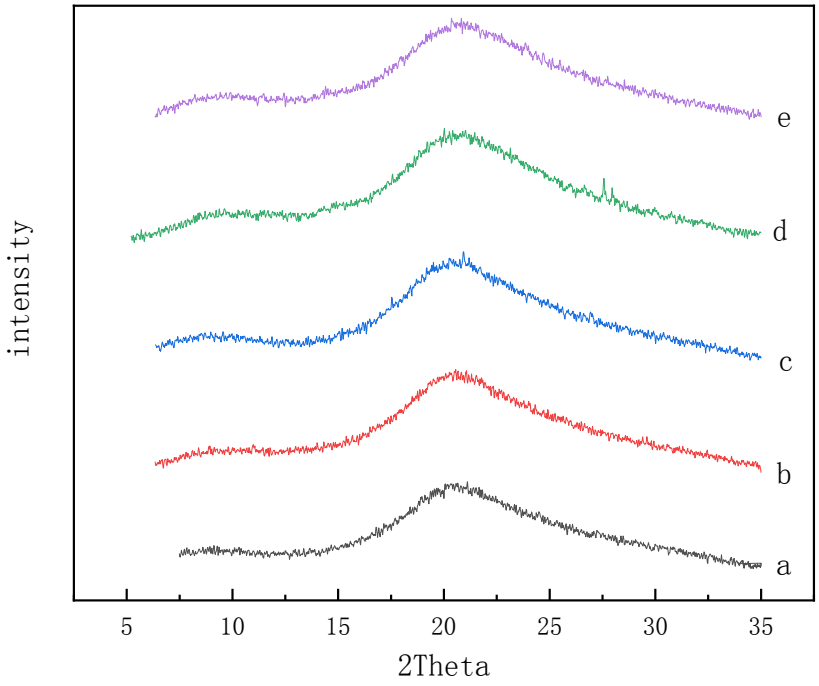

689

690 **Fig. 5: X-ray diffraction of fish myofibrillar protein based composite films with different**

691 **rosemary concentrations (a: FMP/CS, b: FMP/CS/ RE (0.05%), c: FMP/CS/RE (0.10%), d:**

692 **FMP/CS/RE (0.15%), e: FMP/CS/RE (0.20%))**

693

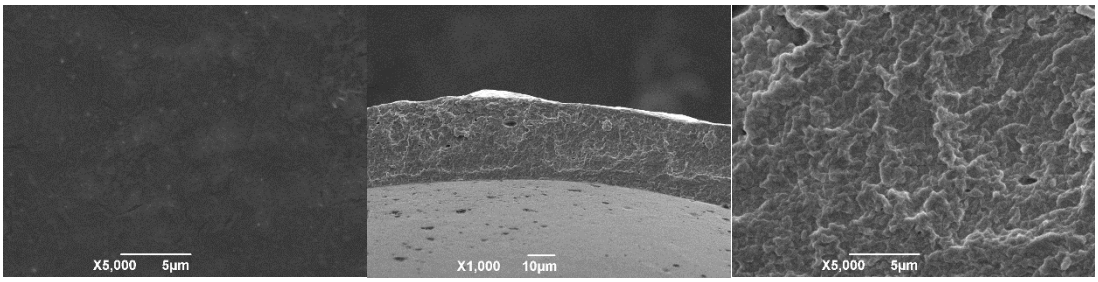

a. FMP/CS composite films

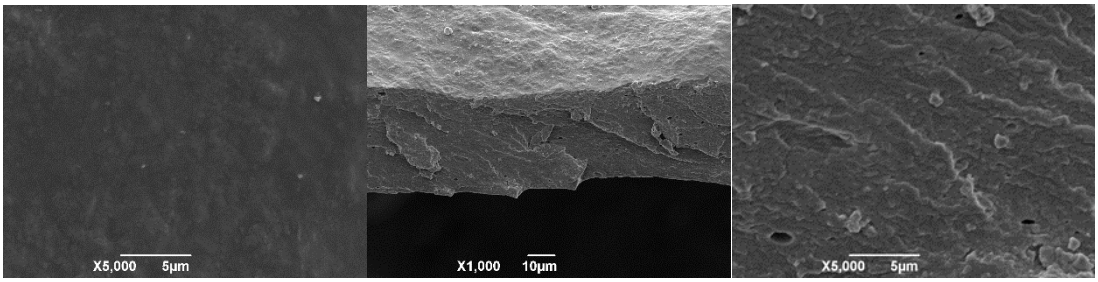

b. FMP/CS/RE (0.05%) composite films

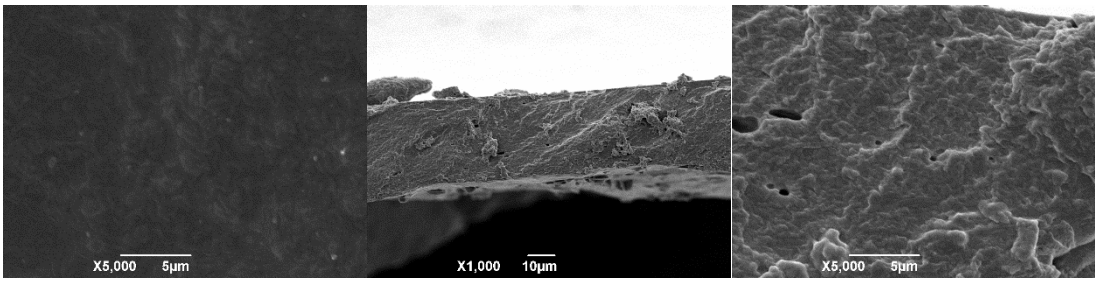

c. FMP/CS/RE (0.10%) composite films

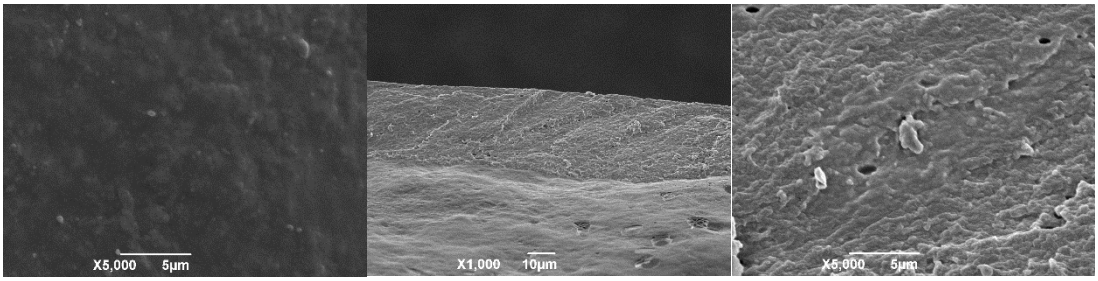

d. FMP/CS/RE (0.15%) composite films

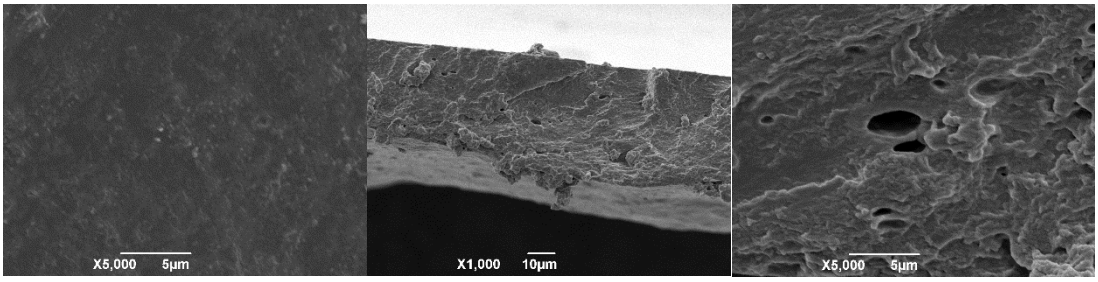

e. FMP/CS/RE (0.20%) composite films

Fig. 6: Scanning electron microscopy (SEM) images of the surface and cross-section of fish

myofibrillar protein based composite films with different concentrations of RE. Surface (5000× magnification), cross section (1000× magnification), cross section (5000× magnification).

710

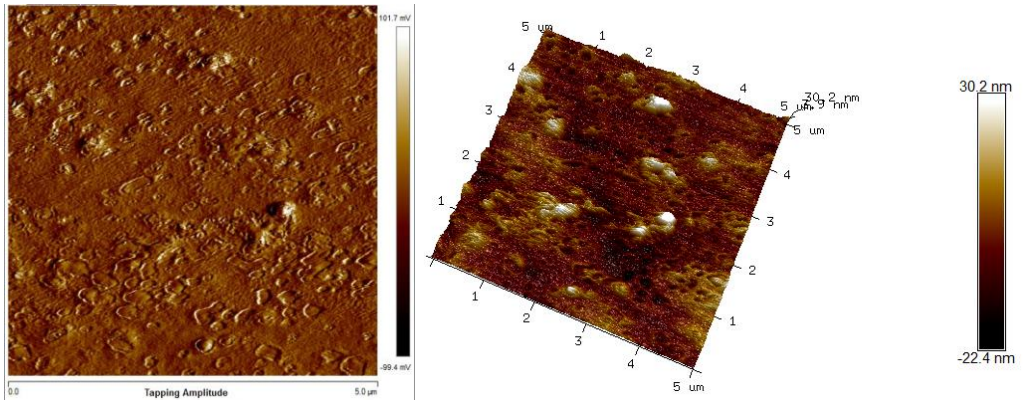

711

712 **a. FMP/CS**

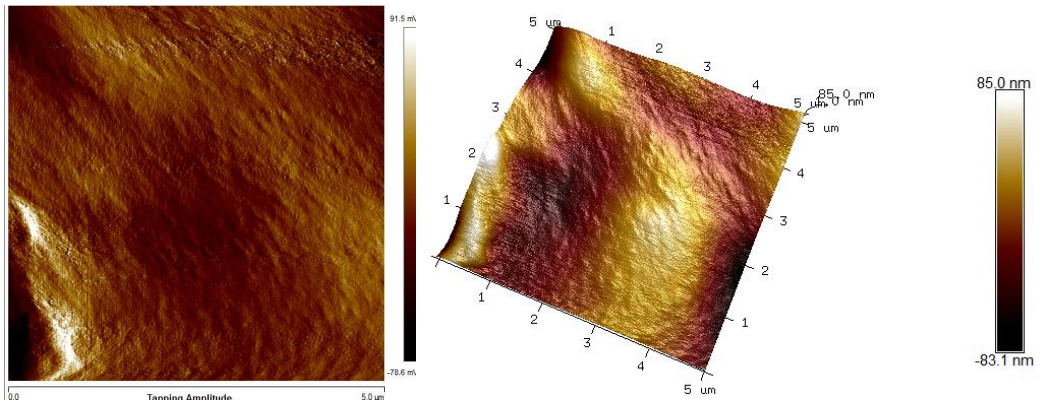

713

714 **b. FMP/CS/RE (0.05%)**

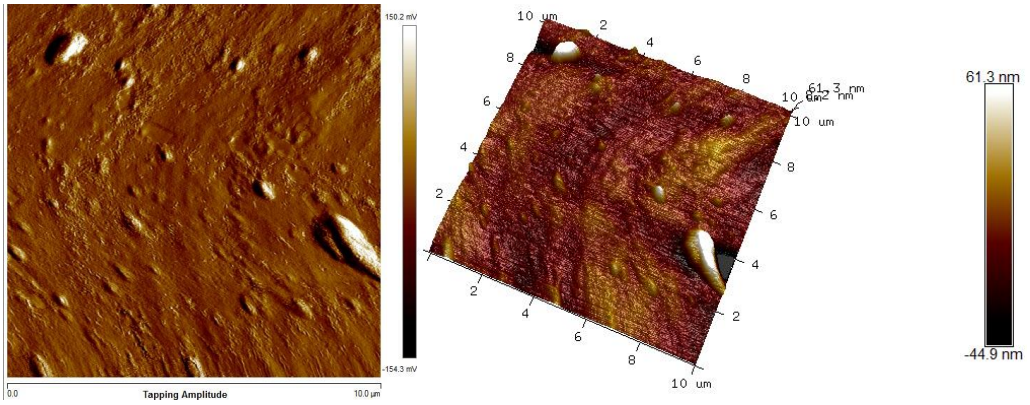

715

716 **c. FMP/CS/RE (0.10%)**

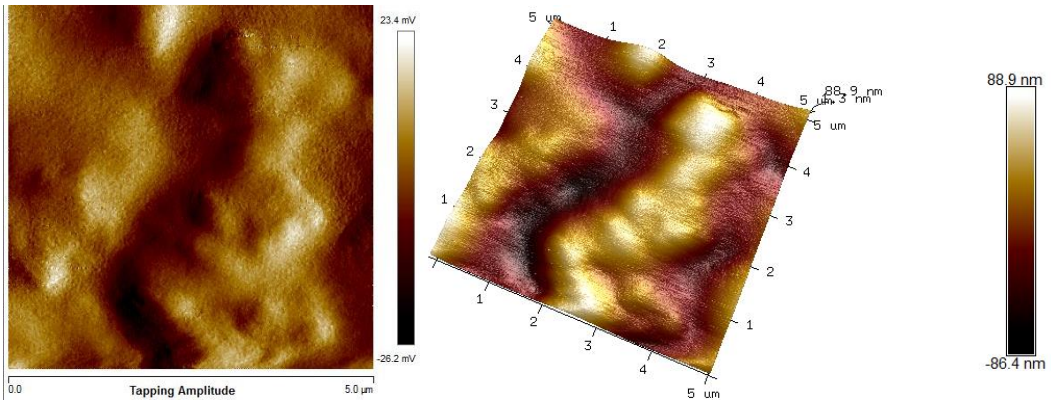

d. FMP/CS/RE (0.15%)

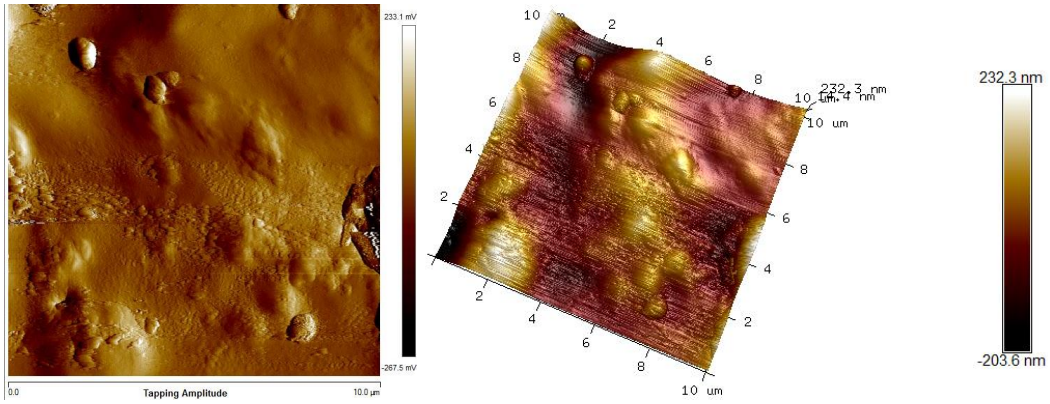

e. FMP/CS/RE (0.20%)

Fig. 7: Surfaces morphology of composite membrane containing different concentrations of rosemary extract （left: 2D, right: 3D）

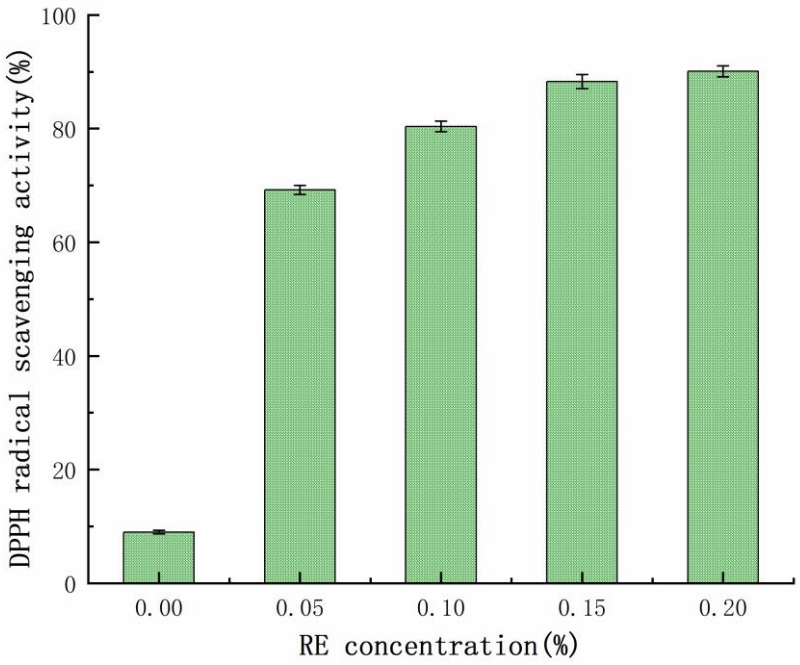

Fig. 8: The DPPH free radical scavenging activity of the composite films containing different concentrations of RE.

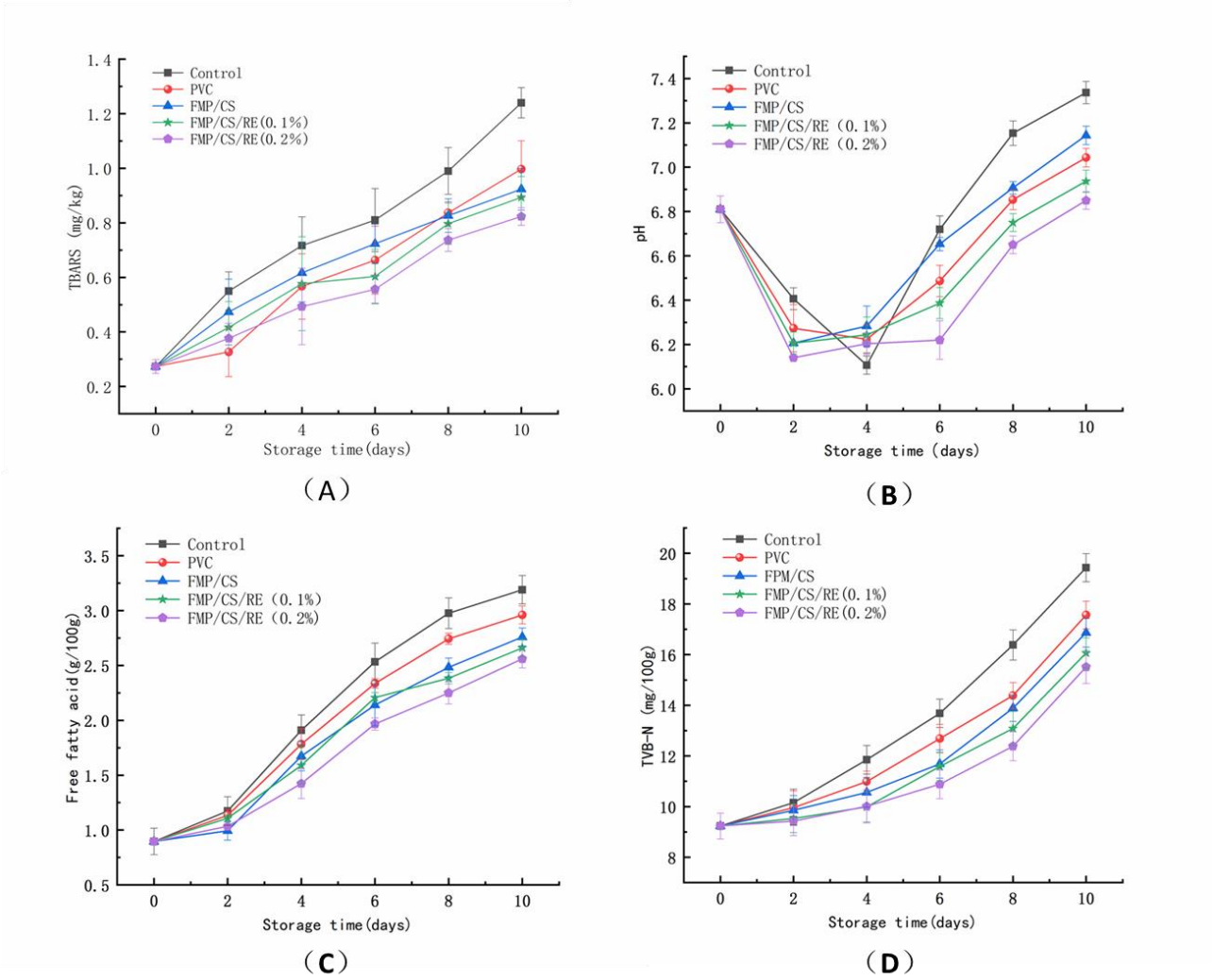

729

730 **Fig. 9: Changes in TBARS, pH, FAA, TVB-N values of grass carp fillets during cold storage.**

731 **(A) TBARS; (B) pH; (C) FAA; (D) TVB-N.**

732

733

734